0.48Tb/s (12x40Gb/s) WDM transmission and high-quality thermo-optic switching in dielectric loaded plasmonics

D. Kalavrouziotis,[1,*] S. Papaioannou,[2,3] G. Giannoulis,[1] D. Apostolopoulos,[1] K. Hassan,[4] L. Markey,[4] J.-C. Weeber,[4] A. Dereux,[4] A. Kumar,[5] S. I. Bozhevolnyi,[5] M. Baus,[6] M. Karl,[6] T. Tekin,[7] O. Tsilipakos,[8] A. Pitilakis,[8] E. E. Kriezis,[8] H. Avramopoulos,[1] K. Vyrsokinos,[3] and N. Pleros[2,3]

[1]*National Technical University of Athens – School of Electrical Engineering and Computer Engineering 9 Iroon Polytechniou Street, Zografou 15780 –Athens, Greece*
[2]*Department of Informatics, Aristotle University of Thessaloniki, Greece*
[3]*Informatics and Telematics Institute, Center for Research and Technology Hellas, Thessaloniki, Greece*
[4]*Institut Carnot de Bourgogne, University of Burgundy, France*
[5]*Faculty of Engineering/Institute of Sensors, Signals and Electrotechnics University of Southern Denmark*
[6]*AMO Gesellschaft für Angewandte Mikro- und Optoelektronik GmbH, Germany*
[7]*Fraunhofer IZM, D-13355 Berlin, Germany*
[8]*Department of Electrical and Computer Engineering, Aristotle University of Thessaloniki*
[*] *dkalav@mail.ntua.gr*

Abstract: We demonstrate Wavelength Division Multiplexed (WDM)-enabled transmission of 480Gb/s aggregate data traffic (12x40Gb/s) as well as high-quality 1x2 thermo-optic tuning in Dielectric-Loaded Surface Plasmon Polariton Waveguides (DLSPPWs). The WDM transmission characteristics have been verified through BER measurements by exploiting the heterointegration of a 60μm-long straight DLSPPW on a Silicon-on-Insulator waveguide platform, showing error-free performance for six out of the twelve channels. High-quality thermo-optic tuning has been achieved by utilizing Cycloaliphatic-Acrylate-Polymer as an efficient thermo-optic polymer loading employed in a dual-resonator DLSPPW switching structure, yielding a 9nm wavelength shift and extinction ratio values higher than 10dB at both output ports when heated to 90°C.

OCIS codes: (250.5403) Plasmonics; (200.4650) Optical interconnects; (250.5300) Photonic integrated circuits.

References and links

1. D. K. Gramotnev and S. I. Bozhevolnyi, "Plasmonics beyond the diffraction limit," Nat. Photonics **4**(2), 83–91 (2010).
2. H. A. Atwater, "The promise of plasmonics," Sci. Am. **296**(4), 56–62 (2007).
3. M. L. Brongersma and V. M. Shalaev, "Applied physics. The case for plasmonics," Science **328**(5977), 440–441 (2010).
4. R. Zia, J. A. Schuller, A. Chandran, and M. L. Brongersma, "Plasmonics: the next chip-scale technology," Mater. Today **9**(7-8), 20–27 (2006).
5. J. A. Dionne, L. A. Sweatlock, M. T. Sheldon, A. P. Alivisatos, and H. A. Atwater, "Silicon-based plasmonics for on-chip photonics," IEEE J. Sel. Top. Quantum Electron. **16**(1), 295–306 (2010).
6. W. L. Barnes, A. Dereux, and T. W. Ebbesen, "Surface plasmon subwavelength optics," Nature **424**(6950), 824–830 (2003).
7. B. Steinberger, A. Hohenau, H. Ditlbacher, A. L. Stepanov, A. Drezet, F. R. Aussenegg, A. Leitner, and J. R. Krenn, "Dielectric stripes on gold as surface plasmon waveguides," Appl. Phys. Lett. **88**(9), 094104 (2006).
8. T. Holmgaard and S. I. Bozhevolnyi, "Theoretical analysis of dielectric-loaded surface plasmon-polariton waveguides," Phys. Rev. B **75**(24), 245405 (2007).
9. J. Gosciniak, V. S. Volkov, S. I. Bozhevolnyi, L. Markey, S. Massenot, and A. Dereux, "Fiber-coupled dielectric-loaded plasmonic waveguides," Opt. Express **18**(5), 5314–5319 (2010).
10. J. Gosciniak, S. I. Bozhevolnyi, T. B. Andersen, V. S. Volkov, J. Kjelstrup-Hansen, L. Markey, and A. Dereux, "Thermo-optic control of dielectric-loaded plasmonic waveguide components," Opt. Express **18**(2), 1207–1216 (2010).

#159585 - $15.00 USD Received 12 Dec 2011; revised 20 Jan 2012; accepted 30 Jan 2012; published 20 Mar 2012

11. K. Hassan, J.-C. Weeber, L. Markey, and A. Dereux, "Thermo-optical control of dielectric loaded plasmonic racetrack resonators," J. Appl. Phys. **110**(2), 023106 (2011).
12. G. Giannoulis, D. Kalavrouziotis, D. Apostolopoulos, S. Papaioannou, A. Kumar, S. I. Bozhevolnyi, L. Markey, K. Hassan, J.-C. Weeber, A. Dereux, M. Baus, M. Karl, T. Tekin, O. Tsilipakos, A. Pitilakis, E. E. Kriezis, K. Vyrsokinos, H. Avramopoulos, and N. Pleros, "Data transmission and thermo-optic tuning performance of dielectric-loaded plasmonic structures hetero-integrated on a silicon chip," Accepted for publication in IEEE Photon. Technol. Lett. 2011.
13. D. Kalavrouziotis, S. Papaioannou, K. Vyrsokinos, A. Kumar, S. I. Bozhevolnyi, L. Markey, J.-C. Weeber, A. Dereux, G. Giannoulis, D. Apostolopoulos, H. Avramopoulos, and N. Pleros, "First demonstration of active plasmonic device in true data traffic conditions: ON/OFF thermo-optic modulation using a hybrid silicon-plasmonic asymmetric MZI," *in Proceedings of OFC/NFOEC Conference* (Los Angeles, CA, USA, 2012), OW3E.3.
14. O. Tsilipakos, T. V. Yioultsis, and E. E. Kriezis, "Theoretical analysis of thermally tunable microring resonator filters made of dielectric-loaded plasmonic waveguides," J. Appl. Phys. **106**(9), 093109 (2009).
15. O. Tsilipakos, E. E. Kriezis, and S. I. Bozhevolnyi, "Thermo-optic microring resonator switching elements made of dielectric-loaded plasmonic waveguides," J. Appl. Phys. **109**(7), 073111 (2011).
16. A. Kumar, J. Gosciniak, T. B. Andersen, L. Markey, A. Dereux, and S. I. Bozhevolnyi, "Power monitoring in dielectric-loaded surface plasmon-polariton waveguides," Opt. Express **19**(4), 2972–2978 (2011).
17. D. A. B. Miller, "Optical interconnects," *in Proceedings of OFC/NFOEC Conference* (San Diego, CA, USA, 2010), Tutorial OThX1.
18. A. Shacham, K. Bergman, and L. P. Carloni, "Photonic networks-on-chip for future generations of chip multiprocessors," IEEE Trans. Comput. **57**(9), 1246–1260 (2008).
19. B. G. Lee, X. Chen, A. Biberman, X. Liu, I.-W. Hsieh, C.-Y. Chou, J. I. Dadap, F. Xia, W. M. J. Green, L. Sekaric, Y. A. Vlasov, R. M. Osgood, Jr., and K. Bergman, "Ultrahigh-bandwidth silicon photonic nanowire waveguides for on-chip networks," IEEE Photon. Technol. Lett. **20**(6), 398–400 (2008).
20. B. G. Lee, A. Biberman, J. Chan, and K. Bergman, "High-performance modulators and switches for silicon photonic networks-on-chip," IEEE J. Sel. Top. Quantum Electron. **16**(1), 6–22 (2010).
21. M. Wu, Z. Han, and V. Van, "Conductor-gap-silicon plasmonic waveguides and passive components at subwavelength scale," Opt. Express **18**(11), 11728–11736 (2010).
22. S. Papaioannou, K. Vyrsokinos, O. Tsilipakos, A. Pitilakis, K. Hassan, J.-C. Weeber, L. Markey, A. Dereux, S. I. Bozhevolnyi, A. Miliou, E. E. Kriezis, and N. Pleros, "A 320Gb/s-throughput capable 2×2 silicon-plasmonic router architecture for optical interconnects," J. Lightwave Technol. **29**(21), 3185–3195 (2011).
23. R. M. Briggs, J. Grandidier, S. P. Burgos, E. Feigenbaum, and H. A. Atwater, "Efficient coupling between dielectric loaded plasmonic and silicon photonic waveguides," Nano Lett. **10**(12), 4851–4857 (2010).
24. J. T. Kim, J. J. Ju, S. Park, M. S. Kim, S. K. Park, and M.-H. Lee, "Chip-to-chip optical interconnect using gold long-range surface plasmon polariton waveguides," Opt. Express **16**(17), 13133–13138 (2008).
25. J. J. Ju, S. Park, M.- Kim, J. T. Kim, S. K. Park, Y. J. Park, and M.-H. Lee, "40 Gbit/s light signal transmission in long-range surface plasmon waveguides," Appl. Phys. Lett. **91**(17), 171117 (2007).
26. J. Bolten, J. Hofrichter, N. Moll, S. Schonenberger, F. Horst, B. J. Offrein, T. Wahlbrink, T. Mollenhauer, and H. Kurz, "CMOS compatible cost-efficient fabrication of SOI grating couplers," Microelectron. Eng. **86**(4-6), 1114–1116 (2009).
27. S. Massenot, J. Grandidier, A. Bouhelier, G. Colas des Francs, L. Markey, J.-C. Weeber, A. Dereux, J. Renger, M. U. Gonzàlez, and R. Quida, "Polymer-metal waveguides characterization by Fourier plane leakage radiation microscopy," Appl. Phys. Lett. **91**(24), 243102 (2007).

1. Introduction

The emergence of plasmonics has been instigated by a great promise for enabling energy-effective and highly integrated optical interconnects [1–6]. Strong mode confinement and the unique capability of natural integration with metal circuitry, enabling highly efficient (electronic) control of waveguide characteristics, are the main attractive features of plasmonic waveguides with respect to bringing down optical circuitry size and power consumption in integrated data interconnect technologies. This potential has triggered remarkable advances in a variety of plasmonic waveguide technologies, with Dielectric-Loaded SPP waveguides (DLSPPW) constituting one of the most promising platforms for enriching the functional portfolio of plasmonics and enabling the penetration of "active" plasmonic circuitry in datacom environments through the utilization of their dielectric loading properties [7–15]. DLSPPW structures employ a dielectric (polymer) material on top of a metallic film, offering in this way an extra interactive mechanism for the control of plasmon propagation [7,8]. This has been highlighted in the recent preliminary experimental [10–13] and theoretical [14,15] studies on the thermo-optic tuning of Polymethylmethacrylate (PMMA)-loaded SPP waveguide structures and on their use for power monitoring purposes [16]. These demonstrations indicate also the enhanced maturity of DLSPPWs compared to other

#159585 - $15.00 USD Received 12 Dec 2011; revised 20 Jan 2012; accepted 30 Jan 2012; published 20 Mar 2012

plasmonic waveguide configurations, rendering them as the most appropriate for taking the next logical step towards their employment in more advanced functional devices.

However, DLSPPWs have so far neither confirmed their ability to sustain signal integrity under realistic high-repetition-rate traffic conditions nor have they allowed for high-quality functional switch performance, as required in real interconnect systems [17–20]. The main reasons for this have been the relatively high propagation losses in the DLSPPW platform along with the limited functional regime available when using solely PMMA as the dielectric loading. Efforts towards counteracting high propagation losses of DLSPPW structures and enabling their communication with the outer world photonic elements have concentrated on their interconnection to lower-loss waveguide platforms [5,12,21–23], still not concluding to a solid proof of their practical application in real high-throughput WDM interconnects. So far, among plasmonic waveguides, only Long-Range SPP (LRSPP) waveguides have been experimentally proven to serve as data transmission lines 24 for up to 40 Gb/s line rates [25], while signal integrity in DLSPPWs has been recently addressed for only 10Gb/s traffic [12]. However, LRSPPs feature significantly weaker mode confinement and more stringent dielectric material limitations (due to the equivalence requirement for upper and lower dielectric layers) as compared to DLSPPWs, negating the circuit size and power consumption advantages envisioned by the introduction of plasmonics. At the same time, work on plasmonic switching using PMMA-loaded thermo-optic structures has revealed the low-energy potential and μsec-scale switching times of DLSPPs when using heterointegration on the SOI waveguide platform [12,13], but switching performance is limited to extinction ratios of a few dBs due to the rather weak thermo-optic efficiency of the PMMA loading.

In this article we present, for the first time to our knowledge, Wavelength Division Multiplexed (WDM)-enabled transmission of Tb/s-scale aggregate traffic through DLSPPWs, reporting on the transfer of twelve 40Gb/s Non-Return-to-Zero (NRZ) modulated data channels through a 60μm-long straight DLSPPW heterointegrated with Silicon-on-Insulator (SOI) waveguides. The solid WDM transmission characteristics of the DLSPPWs are verified through Bit-Error-Rate (BER) measurements showing error-free performance for six out of the twelve channels. Moreover, we demonstrate high-quality DLSPP-based thermo-optic switching by utilizing an efficient thermo-optic polymer as the dielectric loading in a dual-resonator switching fabric. The PMMA loading has been replaced by Cycloaliphatic Acrylate Polymer that exhibits a three times higher thermo-optic coefficient (TOC), enabling in this way enhanced thermo-optic wavelength tuning over 9nm and system-qualified switching performance with more than 10dB extinction ratio values at both output ports when heated up to 90°C. The demonstration of Tb/s-scale WDM data transmission and electrically controlled 1x2 thermo-optic switching with DLSPPW-based components represents a crucial milestone in the development of plasmonic interconnects towards real practical applications.

2. 480 Gb/s WDM transmission experiment and results

We have evaluated the WDM Tb/s traffic transmission characteristics of a 60μm-long straight DLSPPW heterointegrated on a SOI motherboard with silicon rib waveguides and Transverse Mode (TM) grating couplers at both input and output ends, enabling thereby fiber-to-fiber data transmission. The SOI rib waveguide dimensions were 400x340nm^2 with a 50nm-thick remaining slab, while the hosting area of the DLSPPW on the SOI motherboard was etched forming a 200nm-deep recess in the buried oxide (BOX) of the SOI substrate. The DLSPPWs inside the recess comprised a 65nm thick and 3μm wide gold film, on top of which a strip of Polymethylmethacrylate (PMMA) dielectric material with a cross-section of 500x600nm^2 was placed. The integration of plasmonics between the SOI waveguides was based on a butt-coupling approach for interfacing the silicon to the DLSPPWs, which is described in detail in [12].

#159585 - $15.00 USD Received 12 Dec 2011; revised 20 Jan 2012; accepted 30 Jan 2012; published 20 Mar 2012

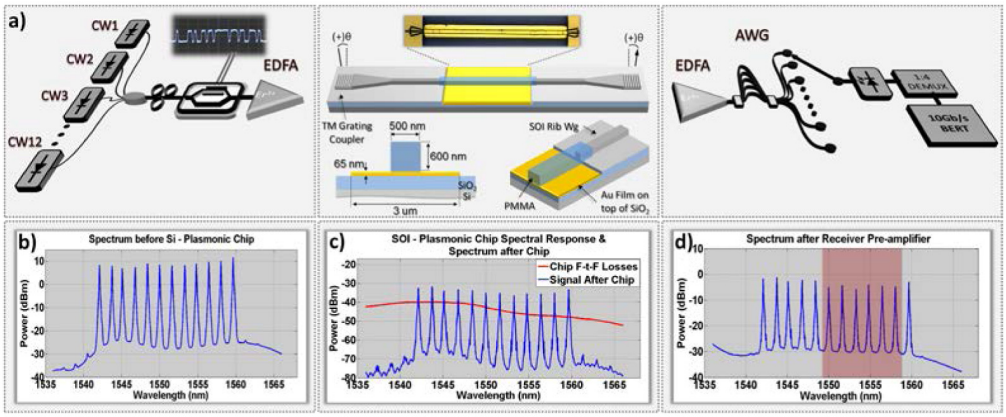

Fig. 1. (a) 480Gb/s WDM Experimental Setup, (b) 12 – Channel Spectrum before entering the chip, (c) 12 – Channel Spectrum directly at the chip's output and Measured Spectral Response of the SOI – Plasmonic chip, (d) 12 – Channel Spectrum after being amplified in the receiver's EDFA

The experimental setup used for the data transmission experiment is depicted in Fig. 1(a). Twelve individual lasers emitting light at wavelengths spaced by 200GHz within the 1542-1560nm spectral window were multiplexed in a common optical fiber and modulated by a 2^{31}-1 Pseudo-Random Bit Sequence (PRBS) at 40Gb/s NRZ line-rate in a 40 GHz Ti:$LiNbO_3$ Mach-Zehnder modulator. The final 12x40Gb/s WDM signal was then amplified by an Erbium-Doped-Fiber-Amplifier (EDFA) chain, providing 24dBm total output power, and launched into a 60-μm-long DLSPPW. The transmission losses of the 60μm long DLSPP waveguide section were found to be 11dB at 1545nm for TM-polarized light, and can be analyzed, based on cutback measurements to 6dB propagation losses and 2.5 dB coupling losses per Si-to-DLSPP interface. The fiber-to-fiber transmission losses of the complete silicon-plasmonic waveguide platform, however, were found to be wavelength dependent ranging between 40dB and 48dB within the 12-channel spectral region. The wavelength dependence and the high value of the fiber-to-fiber losses stem mainly from the two TM grating couplers employed at the chip interfaces that had a coupling loss of 12dB each at 1545nm, while the propagation loss coefficient for the SOI waveguide parts was 4.6dB/cm. The WDM data signal at the output of the chip was amplified and demultiplexed into its constituent wavelengths. Every wavelength was fed then into a high–sensitivity Photo-Receiver followed by an electrical 40:10Gb/s demultiplexer and subsequently connected to a 10Gb/s Error Detector for performing Bit Error Rate (BER) measurements. Figure 1(b), 1(c) and (d) show the 12-channel spectrum before entering the chip, directly at the chip's output, and after being amplified in the receiver's EDFA, respectively, revealing the wavelength dependent behavior of the chip due to the spectral response of its grating couplers, which in turn affects the per-wavelength performance of the final amplification stage.

Figure 2(a) shows the BER curves obtained for all 40Gb/s individual channels after being transmitted through the straight SOI-DLSPPW. Back-to-Back (B2B) measurements were obtained by considering a wavelength-independent, flat reference loss value equal to the fiber-to-fiber chip propagation losses experienced by the spectral region between 1542 and 1548nm, where channels #1-#4 are residing. Error–free operation was obtained for six out of the twelve channels, with their power penalty against the B2B measurements ranging between 0.2 and 1 dB for a 10^{-9} BER value, depending on the spectral position of each specific channel with respect to the TM grating coupler spectral response and the amplification curve of the EDFAs. The remaining six channels (ch#6-#11) that were not promoted by their spectral location exhibited an error-floor at 10^{-7}. The differences in the power penalty values between the error-free performing channels as well as the error-floor operation observed in the other six channels were caused by the wavelength dependent losses of the chip that led

#159585 - $15.00 USD Received 12 Dec 2011; revised 20 Jan 2012; accepted 30 Jan 2012; published 20 Mar 2012

subsequently to wavelength-dependent Optical Signal-to-Noise Ratio (OSNR) values and different signal

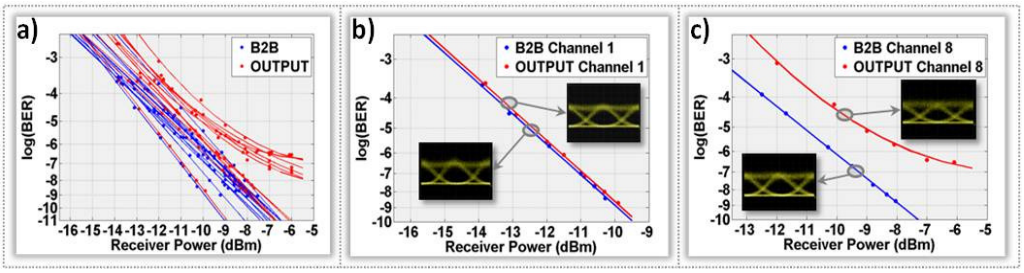

Fig. 2. (a) BER curves for all 40Gb/s B2B and transmitted channels, and BER curves and Eye Diagrams for (b) channel #1 (Best – Performing Channel) and (c) channel #8 (Worst – Performing Channel)

degradation levels per channel in the output EDFA stage. Though this could have been in principle avoided by demultiplexing the WDM signal prior amplification, this was prohibited by the low output power per channel obtained at the chip's output, which was lower than the input power limit of the available pre-amplification stages. The 24dBm total power level of the WDM signal at chip's input and the high fiber-to-fiber losses resulted to a WDM signal output power of only −20dBm being marginally above the operational input power requirements of the output amplifier, necessitating the use of a common EDFA at the chip output for amplifying the entire 12-channel signal. To this end, the obtained error-floors can be negated either by selecting all channel wavelengths to reside within the flat spectral response region of the chip or, alternatively, by employing optimized WDM amplification stages and using lower loss TM grating coupler [26] so as to allow for more efficient in and out coupling.

Figure 2(b) and 2(c) depict the BER curves and the corresponding eye diagrams for the best and worst performing channels #1 and #8, respectively, providing a more detailed look into the performance of the individual channels. Ch#1 exhibits a power penalty of only 0.2dB, while ch#8 has an error-floor at 10^{-7} as a result of the enhanced noise level accumulated in the output EDFA due to the almost 8dB higher losses experienced by this channel compared to its respective B2B evaluation. It should be noted that a similar power penalty value of only 0.2dB was obtained for all 40Gb/s channels when being evaluated individually in single-channel transmission conditions through the SOI-DLSPPW platform, close to the respective power penalty value reported for 10Gb/s single-channel transmission [12]. In the single-channel transmission analysis, the B2B reference loss value was always selected to equal the chip propagation losses experienced by the specific wavelength channel being under investigation.

3. Thermo-optic tuning experiment and results

Besides broadband WDM data carrying credentials, the utilization of DLSPPW modules in functional applications like switching and routing circuitry [22] requires "active" DLSPP-based structures with high-quality extinction ratio metrics. This has been accomplished by means of a thermo-optic dual-resonator DLSPPW platform where PMMA loading has been replaced by Cycloaliphatic Acrylate polymer that exhibits higher thermo-optic coefficient (TOC) enabling in this way enhanced thermo-optic wavelength tuning properties and system-qualified switching performance.

The integration of the new polymer was based on the deposition of 600nm thick layers, realized by spin coating the UV-curable cycloaliphatic acrylate resin diluted in PGMEA in proportions 2:3 at 2000 rpm, on top of the 3mm wide and 60nm thick gold layer of a metalized glass substrate. The films were processed with 250nm deep UV lithography using a Süss-Microtech MJB4 mask aligner in the vacuum contact mode and a commercial mask

#159585 - $15.00 USD Received 12 Dec 2011; revised 20 Jan 2012; accepted 30 Jan 2012; published 20 Mar 2012

(Photronics Inc. Dresden) with negative structures, due to the negative-tone behavior of the material, in order to form the 500x600nm^2 waveguides of the dual resonator structure. Measurements of the refractive index and the TOC of 250nm UV-cured cycloaliphatic acrylate polymer films were obtained in the 300nm-to-800nm spectral range, using a Jobin-Yvon ellipsometer with 75° incidence angle. Extrapolation of data in the IR telecom spectral

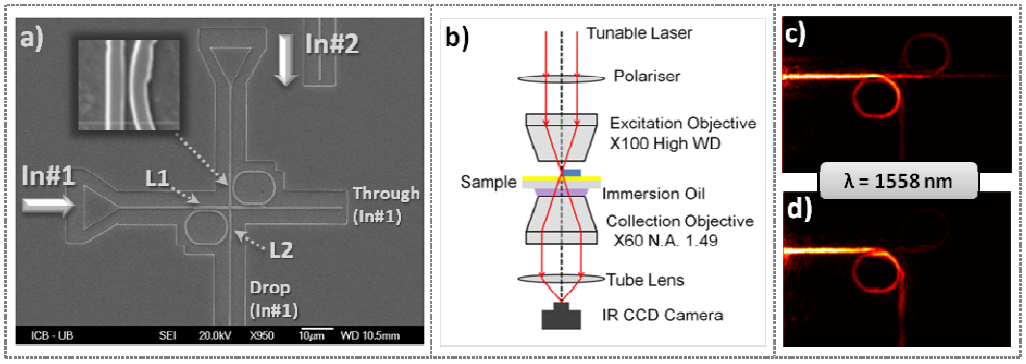

Fig. 3. (a) SEM image of the dual-resonator Cycloaliphatic Acrylate Polymer-loaded DLSPPW switch, (b) Leakage Radiation Microscopy (LRM) Setup, LRM image in (c) "Cool" and (d) "Hot" state at λ = 1558nm

range (up to 1600nm) has been performed on the basis of a Cauchy model describing the spectral dependence of the index of refraction, leading to 1.53 refractive index, at λ = 1.55μm, and TOC varying between −2.9 and $-3\text{x}10^{-4}(°\text{C}^{-1})$, that is approximately three times higher than in the case of PMMA.

Figure 3(a) shows a Scanning Electron Microscope (SEM) image of the fabricated DLSPPW switch, illustrating the dual-resonator layout that comprises two perpendicularly intersecting DLSPPWs along with two diagonally positioned identical DLSPPW racetrack resonators, having R = 5μm radius and two straight waveguide region lengths of L_1 = 2μm and L_2 = 0μm respectively. The image's inset reveals the adequate quality of the DLSPPW structures with the polymer-loaded waveguides exhibiting a nearly square 500x600nm^2 cross section, allowing for a gap resolution of 300nm between the intersecting waveguides and the racetrack resonators. The temperature elevation mechanism was provided by connecting the underlying gold film to a current source capable of delivering a maximum current of 400mA and temperature variations were monitored through a micro-thermocouple-isolated residing on the gold surface.

The spectral response of this device was recorded using Leakage Radiation Microscopy (LRM), since this structure was not heterointegrated on a SOI platform making it impossible to employ fiber-coupling-based characterization processes. Leakage Radiation Microscopy is a well known method used to collect the radiation of the leaky DLSPPW modes propagating along the structure. The LRM setup used for the measurements is shown in Fig. 3(b) and more details about its operation can be found in [11,27]. Figures 3(c) and 3(d) illustrate the respective LRM images obtained at 1558nm both at room temperature ("cool" state) and at its "hot" state, respectively, which corresponds to a DC injected current value of 400mA and a temperature change of ΔT = 60±5 K. Successful change of the device's switching state can be clearly observed, with the signal exiting the device through its Through-port when being in "cool" state and emerging at its Drop-port when turning to "hot" state.

The transmission spectra for both through and drop output ports of the DLSPPW dual-resonator switch are shown in Fig. 4(a) and 4(b), respectively, when the DLSPPW mode is excited at In#1 port, again for both its "cool" and "hot" operational states. A clear resonant behavior can be observed with the Free Spectral Range (FSR) of the through-port resonances being equal to 38nm. When operating in unheated conditions, the resonant dips at the through-port have an Extinction Ratio (ER) of more than 35dB, while the corresponding ER

#159585 - $15.00 USD Received 12 Dec 2011; revised 20 Jan 2012; accepted 30 Jan 2012; published 20 Mar 2012

value for the Drop-port resonant peak between 1560 and 1580nm is close to 10dB. Insertion losses (IL) for the through and drop port, measured at the maximum of each transfer function, are 10dB and 8dB, respectively. The quality factor of the switch was calculated to be ~80 for the through and ~82 for the drop port at the resonance wavelengths of 1568 and 1572nm, respectively, and the propagation loss factor of the DLSPPW was measured to be 0.1dB/μm. By raising the temperature of the polymer strip to 90°C, a wavelength shift of 9nm is observed at both

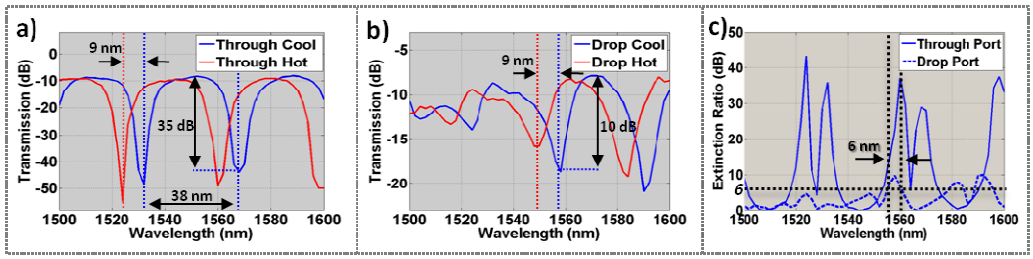

Fig. 4. (a) Transmission spectra for "Through" output port in "Cool" and "Hot" state, (b) Transmission spectra for "Drop" output port in "Cool" and "Hot" state, (c) Extinction Ratio values between "Cool" and "Hot" switching states at "Through" and "Drop" outputs

through- and drop-port resonances as a result of the thermo-optically induced phase shift experienced during propagation in the dual-resonator setup.

Figure 4(c) presents the ER values obtained between "cool" and "hot" switching states at both output ports and over the complete 1500-1600nm spectral window, revealing clearly high-quality 1x2 thermo-optic tuning with 23dB and 10dB ER at through and drop-outputs, respectively, at 1558nm. ER values higher than 6dB are obtained over a 6nm spectral range around 1558nm for both output ports, confirming the broadband switching characteristics of the realized DLSPPW switch that can allow in principle for simultaneous switching of six 100 GHz-spaced WDM channels. The 6dB over 6nm range ER values are similar to the performance of silicon-based switches employed in WDM routing platforms 20, however the DLSPPW layout requires a significantly lower footprint while providing this ER over multiple 100GHz-spaced channels.

It should be noted that this configuration provides high ER values simultaneously at both its output ports and the highest among all ring -or racetrack- resonator-based thermo-optic plasmonic structures, forming in this way the first high-quality 1x2 plasmonic thermo-optic element. This owes both to its dual-resonator layout as well as to its higher thermo-optic effectiveness stemming from its Cycloaliphatic Acrylate polymer loading, given that the maximum wavelength shifting in PMMA-loaded SPP devices is lower than 7nm for the same level of induced temperature change [11,12]. The high level of driving current required for heating owes to the relatively large underlying gold film dimensions and can be certainly reduced by adopting DLSPP fabrication schemes compatible to DLSPP-on-SOI heterointegration processes [12], allowing for similar temperature changes with just a few tens of mAs and for power consumption requirements as low as a few mWs [12].

4. Summary

We have demonstrated the WDM transmission of 0.48 Tb/s aggregate traffic through SOI-integrated DLSPPWs and high-quality 1x2 thermo-optic switching in the Cycloaliphatic-Acrylate-Polymer-loaded DLSPPW dual-resonator layout. The results obtained confirm for the first time the WDM signal integrity credentials of the DLSPPW platform and provide a solid proof of its WDM data supportive application perspectives. In addition, they verify the enhanced thermo-optic tuning performance of plasmonic switching structures when replacing the PMMA-loading with Cycloaliphatic-Acrylate polymer. Taking into account the μs-scale switching speed characteristics of PMMA-loaded thermo-optic devices [13], the high ER performance of the novel 1x2 thermo-optic plasmonic element demonstrates the strong

#159585 - $15.00 USD Received 12 Dec 2011; revised 20 Jan 2012; accepted 30 Jan 2012; published 20 Mar 2012

potential for DLSPPs to serve as high-quality switch configurations in true data routing applications. To this end, these results pave the inroad towards high-quality active plasmonic modules performing in true WDM data interconnect environments and requiring low power consumption requirements, when combined with SOI heterointegration concepts [12].

Acknowledgment

This work was partially supported by the European FP7 ICT-PLATON (ICT- STREP no. 249135) project.

#159585 - $15.00 USD Received 12 Dec 2011; revised 20 Jan 2012; accepted 30 Jan 2012; published 20 Mar 2012